Marine Chemistry 194 (2017) 146–157

Contents lists available at ScienceDirect

Marine Chemistry

journal homepage: www.elsevier.com/locate/marchem

Coupled ultrafiltration and solid phase extraction approach for the targeted study of semi-labile high molecular weight and refractory low molecular weight dissolved organic matter

Taylor A.B. Broek[a,b,*], Brett D. Walker[c], Thomas P. Guilderson[a,b], Matthew D. McCarthy[a]

[a] University of California, Ocean Sciences Department, 1156 High Street, Santa Cruz, CA 95064, USA
[b] Lawrence Livermore National Laboratory, Center for Accelerator Mass Spectrometry, 7000 East Avenue, Livermore, CA 94550, USA
[c] University of California, Department of Earth Systems Science, 2212 Croul Hall, Irvine, CA 92697, USA

ABSTRACT

Only a small fraction of dissolved organic matter (DOM) can be characterized at the molecular level by direct seawater analysis. Thus, the study of DOM requires isolation of extremely dilute organics from orders of magnitude greater concentrations of inorganic salts. Traditional isolation approaches have sought to isolate representative DOM fractions, however, currently available isolation methods all have selective chemical or physical biases. Recent work has indicated that DOM exists in a functional continuum of molecular size and ^{14}C age. High molecular weight (HMW) DOM is primarily composed of younger, semi-labile material, while much older, low molecular weight (LMW) DOM dominates the refractory background pool. Here we describe a new large volume DOM isolation approach that selectively isolates HMW and LMW DOM fractions with distinct ^{14}C ages, a proxy for reactivity. The method uses ultrafiltration (UF) to isolate HMW DOM (UDOM), and then solid phase extraction (SPE) to isolate LMW DOM permeating the UF system. We first assess two SPE sorbents (Agilent Bond Elute PPL and Diaion HP-20) for DOM chemical and isotopic selectivity. Second, we evaluate our UF/SPE approach in the context of DOM recovery, elemental (C/N) and isotopic ($\delta^{13}C$, $\delta^{15}N$, $\Delta^{14}C$) composition of 8 HMW and LMW sample pairs, isolated from the North Central Pacific Ocean. Radiocarbon ($\Delta^{14}C$) analysis shows major differences in the $\Delta^{14}C$ value of HMW ($\Delta^{14}C = -37$ to -380‰) and LMW ($\Delta^{14}C = -343$ to -578‰) DOM fractions. We also observe elemental and stable isotopic offsets between HMW and LMW DOM at all depths. HMW UDOM (C/N = 11.5 to 13.1, $\delta^{13}C = -22.5$ to -21.1‰, $\delta^{15}N = 6.2$ to 7.1‰) has significantly lower C/N ratios and higher $\delta^{13}C$ and $\delta^{15}N$ values than LMW SPE-DOM (C/N = 24.2 to 28.5, $\delta^{13}C = -23.3$ to -22.2‰, $\delta^{15}N = 3.1$ to 4.0‰), with the exception of surface $\delta^{13}C$, which is equivalent in both size fractions. Together, these results indicate that our combined UF/SPE method successfully isolates separate young (semi-labile, HMW) and old (refractory, LMW) DOM fractions, each with distinct chemical and isotopic composition. Ultimately, by limiting the influence of DOM reactivity mixtures, our method provides an alternative approach for understanding DOM sources and cycling.

1. Introduction

Marine dissolved organic matter (DOM) represents the largest pool of actively cycling carbon and nitrogen in the ocean. The amount of carbon contained within ocean DOM is comparable in size to atmospheric CO_2, and therefore represents a major global reservoir, capable of altering atmospheric CO_2 levels if the balance of sources and sinks is substantially altered. Despite its importance in global biogeochemical cycles, it has remained difficult to characterize DOM at the molecular level. Only a small fraction of DOM exists as identifiable biomolecules, and most techniques for studying DOM composition require the isolation of dilute organics from high concentrations of inorganic salts (Benner, 2002).

Historically, DOM isolation methods have focused on maximizing recovery efficiency in order to isolate representative material at quantities sufficient for sample-intensive molecular and spectroscopic characterization approaches (Mopper et al., 2007). For example, solid phase extraction (SPE) using hydrophobic sorbents such as XAD and C_{18} recovers 20–50% of marine DOM. However, this approach is chemically selective, and the isolated material (SPE-DOM) is strongly biased against polar molecules (Amador et al., 1990; Green and Blough, 1994; Schwede-Thomas et al., 2005; Simjouw et al., 2005). As such, this SPE-

* Corresponding authors at: University of California, Ocean Sciences Department, 1156 High Street, Santa Cruz, CA 95064, USA.
E-mail address: tborrius@ucsc.edu (T.A.B. Broek).

http://dx.doi.org/10.1016/j.marchem.2017.06.007
Received 12 January 2017; Received in revised form 14 June 2017; Accepted 22 June 2017
Available online 23 June 2017
0304-4203/

DOM is poorly representative of total DOM (e.g., Town and Powell, 1993). New generations of hydrophobic styrene-divinylbenzene polymer based SPE sorbents have gained popularity for DOM isolation, generally achieving higher recovery efficiency than previous SPE (40 to 80%), with less reported molecular selectivity (Chen et al., 2016; Coppola et al., 2015; Dittmar et al., 2008; Green et al., 2014; Medeiros et al., 2015a; Stubbins et al., 2012). However, relative to total DOM, this SPE-DOM is C-rich, primarily low molecular weight (LMW), and has slightly older average ^{14}C ages, suggesting that it too is not entirely representative of the total DOM pool (Coppola et al., 2015; Dittmar and Stubbins, 2014; Green et al., 2014).

Tangential flow ultrafiltration (UF) is another approach that has been widely used to isolate DOM (Benner, 2002; Benner et al., 1997; Guo et al., 1996; Santschi et al., 1995; Walker et al., 2011). UF uses semi-permeable membranes to retain only high molecular weight (HMW) DOM (UDOM). Whereas UDOM has C/N ratios similar to total DOM, it is dominated by a major reactive heteropolyscharide component (Aluwihare et al., 1997; Benner et al., 1997). In addition, the average ^{14}C age of UDOM is significantly younger than total DOC (Loh et al., 2004; Santschi et al., 1995; Walker et al., 2011, 2014), especially in the surface ocean. Further, most marine DOM (60–90%) is LMW (< 1 kDa), and readily permeates a UF system (Benner and Amon, 2015).

Due to the operational nature of these isolation techniques, neither UDOM nor SPE-DOM is particularly representative of the total DOM pool. To date, no method consistently isolates total DOC across ocean depths and water masses, with most methods achieving substantially < 100% recovery. More problematic than absolute recovery, however, is that all isolations suffer from varying degrees of selectivity. Incomplete recoveries and the inherent biases associated with different isolation mechanisms (size, hydrophobicity, etc.), can lead to broad process interpretations based on isolated sub-fractions, which likely represent very different compositional and functional DOM components.

Recent research suggests that a new approach to DOM isolation, focused on selective isolation of separate old and young fractions, may be more useful in investigating DOM composition and cycling. Specifically, multiple studies note trends in DOM composition, ^{14}C age, and reactivity, which are strongly linked to nominal molecular size (Benner and Amon, 2015; Walker et al., 2011, 2016a, 2016c). In general, HMW DOM is more biologically labile, biopolymer-rich, with younger ^{14}C ages, more identifiable biochemicals, and greater reactivity. In contrast, LMW DOM is generally more biologically recalcitrant, contains far fewer identifiable biomolecules, and has older ^{14}C ages at all depths (Amon and Benner, 1996, 1994; Benner et al., 1997; Benner and Amon, 2015; Kaiser and Benner, 2009; Walker et al., 2016c, 2016a, 2014, 2011). These observations expand upon the classical "two-pool" model of DOC cycling (Druffel et al., 1992; Williams and Druffel, 1987). In the two-pool model, a homogenous pool of "background" refractory DOM is present throughout the ocean, and is comprised of DOM with old ^{14}C ages (Beaupré and Aluwihare, 2010; Mortazavi and Chanton, 2004). Superimposed upon this background, refractory DOM is a pool of surface produced, "excess", semi-labile material with young ^{14}C ages (Carlson and Hansell, 2014; Walker et al., 2016c, 2011).

Here we evaluate a new DOM isolation approach, sequentially combining UF and SPE, in order to target two distinct, operationally defined DOM pools. The average MW of DOM retained by UF is a function of the concentration factor used (CF; ratio of volume filtered to final retentate volume), a high CF results in the retention of higher MW material (Kilduff and Weber, 1992; Walker et al., 2011). This UF attribute allows for the targeted isolation of not only higher MW material, but also DOM with younger average ^{14}C ages (Walker et al., 2011). The DOM permeating a UF system is by definition LMW. Therefore, we hypothesize that SPE of seawater UF permeate will allow for the targeted isolation of LMW, refractory, background DOM.

We first test two formulations of SPE sorbent to evaluate the properties of SPE isolated material relative to total seawater DOM. We then apply our full UF/SPE method to selectively isolate HMW and LMW DOM from the surface to deep-ocean in the Central North Pacific Subtropical Gyre (NPSG). Finally, we evaluate our approach by comparing the elemental ratios (C/N), stable isotopic ($\delta^{13}C$, $\delta^{15}N$), and radiocarbon ($\Delta^{14}C$) properties of individual HMW and LMW DOM isolates. Overall, our main objective is not to optimize total DOM recovery, but rather to develop a method that can isolate large quantities of distinct operational fractions having bulk properties consistent with either semi-labile (excess) or refractory (background) DOM.

2. Materials and methods

2.1. Definitions

Here we define "total DOM" to be all DOM passing a 0.2 μm filter. "HMW UDOM" represents the ≥ 2.5 kD material retained by the UF system. "SPE-DOM" represents material retained by the SPE sorbents. In the SPE sorbent comparison section, "PPL SPE-DOM" and "HP-20 SPE-DOM" are used to refer to DOM extracted from 0.2 μm-filtered seawater by PPL and HP-20 SPE sorbents respectively. To distinguish SPE-DOM isolates of 0.2 μm-filtered seawater from material collected from ≤ 2.5 kD UF permeate using the combined UF/SPE method, we use "LMW SPE-DOM" for the ≤ 2.5 kD fraction. DOC and DON are used when discussing C or N specific properties of the DOM fractions.

2.2. Sample collection

Samples were collected on two separate research cruises aboard the R/V Kilo Moana in August 2014 and May 2015. Sampling was conducted at the Hawaii Ocean Time Series Station ALOHA (A Long-Term Oligotrophic Habitat Assessment; 22° 45′N, 158° 00′W).

Significant precautions were taken to ensure ^{14}C–tracer free shipboard sampling. All laboratory spaces were cleaned floor-to-ceiling with 10% HCl followed by ethanol. Exposed surfaces (bench tops, walls, and ceiling) were covered and air vents redirected using plastic sheeting. ^{14}C swabs of lab spaces, outside deck areas, and sampling equipment measured during scheduled shipboard contamination monitoring swab tests by the University of Miami tritium laboratory (http://www.rsmas.miami.edu/groups/tritium) were reviewed prior to each cruse. More sensitive ^{14}C swipes were taken throughout the ship before and after each cruise and analyzed by accelerator mass spectrometry (AMS) to confirm a ^{14}C–tracer free sampling environment.

Surface water was sampled via the vessel's underway sampling system. The intake pipe is situated on the forward starboard hull section of the vessel approximately 7.5 m below the waterline. The laboratory seawater tap was allowed to flush for 2 h prior to each sampling. Seawater was pre-filtered through 53 μm Nitex mesh, and pumped through a 0.2 μm polyethersulfone (PES) cartridge filter (Shelco Filters, Micro Vantage, water grade, 9.75″ DOE, polycarbonate housing) prior to introduction to the ultrafiltration system. Large volume subsurface water samples were collected using successive casts of a rosette equipped with 12 × 24 L Niskin bottles. Sample water was transferred from the Niskin bottles via platinum cured silicone tubing to sample rinsed fluorinated high density polyethylene (F-HDPE) carboys which were subsequently emptied into 1000 L HDPE intermediate bulk containers for storage. Subsurface water was similarly pumped through a 0.2 μm PES cartridge filter prior to ultrafiltration. All filters and storage containers were cleaned with 10% HCl prior to contact with sample seawater.

2.3. Experimental design

Total DOM was separated into two distinct size fractions using a sequential combination of UF and SPE. A flow diagram of the isolation

protocol is shown in Fig. 1. HMW UDOM was first isolated using a large-volume UF system; the permeate stream of this system (containing LMW DOM able to pass the UF membranes) was then collected, acidified in large batches to pH 2 and passed through the SPE sorbent. The eluted material from the SPE sorbent represents the LMW SPE-DOM fraction.

2.4. Tangential-flow ultrafiltration

The main UF system was constructed using a modified design of the system described in Roland et al. (2009), and expanded on by Walker et al. (2011). Briefly, the system was comprised of four-spiral wound PES UF membranes, having a nominal molecular weight cut off of 2.5 kD (GE Osmonics GH2540F30, 40-inch long, 2.5-inch diameter). The membranes were mounted in stainless steel housings, plumbed in parallel to a 100 L fluorinated HDPE reservoir, with flow driven by a 1.5 HP stainless steel centrifugal pump (Goulds Pumps, Stainless steel centrifugal pump, NPE series 1 × 1–1/4–6, close coupled to a 1–1/2 hp, 3500 RPM, 60 Hz, 3 phase, Open Drip Proof Motor; 5.75 Inch Impeller Diameter, Standard Viton Mechanical Seals). All other system plumbing components contacting seawater were composed of polytetrafluoroethylene (PTFE) or stainless steel.

The system was run continuously at a membrane pressure of 40–50 psi, resulting in permeation flow rates of 1–2 L/min, depending primarily on the temperature of the feed seawater. Sample water was fed into the system using peristaltic pumps and platinum cured silicone tubing at a flow rate matched to the system permeation rates to ensure a constant system volume of approximately 100 L.

Seawater samples of 3000–4000 L were concentrated to a final retentate volume of 15–20 L, drained from the system into acid washed PC carboys and refrigerated (< 12 h at 2 °C) until the next phase of processing. Samples requiring storage for longer than 12 h were frozen and stored at − 20 °C. The UF system was then reconfigured to a smaller volume system, consisting of a single membrane having a smaller nominal molecular weight cutoff (GE Osmonics GE2540F30, 40-inch long, 2.5-inch diameter, 1 kD MWCO), and a 2.5 L PES reservoir for further volume reduction and subsequent salt removal (diafiltration). Using this smaller system, samples were reduced to 2–3 L under lower pressure (25 psi, permeation rate = 250 mL/min). Samples were then diafiltered using 40 L of 18.2 MΩ Milli-Q (ultrapure) water, adding water to the sample retentate reservoir at the same rate of membrane permeation. Reduced and diafiltered samples were stored in acid washed PC bottles at − 20 °C for transport. In the laboratory, samples were further concentrated by rotary evaporation using pre-combusted glassware (450 °C, 5 h). A molecular sieve and a liquid nitrogen trap were placed between the vacuum pump and rotovap chamber to ensure no contamination of isolated material by back streaming of hydrocarbons or other contaminants. After reduction to 50–100 mL, samples were dried to powder via centrifugal evaporation in PTFE centrifuge tubes. Dry material was homogenized with an ethanol cleaned agate mortar and pestle, transferred to pre-combusted glass vials, and stored in a desiccation cabinet until subsequent analyses.

2.5. Solid phase extraction

Solid phase extraction was conducted using PPL sorbent (Agilent Bondesil PPL, 125 µm particle size, part # 5982-0026) following the general recommendations of Dittmar et al. (2008) and Green et al. (2014), including loading rates, seawater to sorbent ratios, and elution volumes and rates. Between 300 and 500 g of sorbent was used for each extraction, depending on sample volume and DOC concentration, with average loading of 4.2 ± 1.4 L UF permeate per g sorbent representing 1.9 ± 0.6 mg DOC per g sorbent or a DOC to sorbent mass ratio of 1:600 ± 200. This is in line with both the recommendations of Dittmar et al. (2008) and recent recommendations of Li et al. (2016). Permeate from the UF system was fed through PTFE tubing to a pair of 200 L HDPE barrels. The permeate water was then acidified in 200 L batches to pH 2 by adding 400 mL of 6 M HCl (Fisher Chemical, ACS Plus grade). Batch samples were mixed continuously during collection, acidification, and loading using a peristaltic pump and platinum cured Si and PTFE tubing positioned at the surface and bottom of each barrel. Acidified batches of seawater permeate were then pumped through the SPE sorbent. SPE flow rates were matched to UF permeation rates (1–2 L/min), such that a pair of 200 L barrels allowed one barrel to be filled while the contents of the other was passed through the sorbent.

Three custom SPE column configurations were used to contain the sorbent material. The column configuration was modified several times for ease of use on subsequent cruises. First, an open, gravity fed, large (49 mm ID × 1000 mm length, 1875 mL volume) glass chromatography column with 40 µm fritted disk and PTFE stopcock (Kimble-Chase™, Kontes™) was used. Next, we tested a custom built high-pressure SS housing (10 cm ID × 3.5 cm bed height), and finally a parallel combination of 2 medium-pressure glass chromatography columns (Kimble-Chase™, Kontes™, Chromaflex LC, 4.8 mm ID × 30 cm, 543 mL volume). While all designs proved to be functionally equivalent, the latter parallel combination of 2 medium-pressure glass columns ultimately provided the best configuration in order to maximize flow rates while simultaneously optimizing the ratio of sorbent bed height to loading speed. Further, the commercial availability and ease of use associated with this configuration made it our preferred design.

Following sample loading, the SPE sorbent was desalted with 6 L of pH 2 ultrapure water at a low flow rate (250–300 mL/min). After desalting, the SPE sorbent was transferred to a glass chromatography column (75 mm ID × 300 mm length, 40 µm fritted disk, PTFE stopcock) with ultrapure water rinses to ensure quantitative transfer. Isolated organic material was then eluted from the sorbent with five to six 500 mL additions of methanol. The secondary all-glass and PTFE column was used to insure that all wetted parts had strong chemical resistance to the methanol used during DOM elution. The eluted methanol solution was stored in pre-combusted amber glass bottles at − 20 °C for transport. Similar to UF samples, the methanol-eluted solutions were first reduced by rotary evaporation to 50–100 mL. Samples were then dried to powder via centrifugal evaporation in PTFE centrifuge tubes. Dry material was homogenized with an ethanol cleaned agate mortar and pestle, transferred to pre-combusted glass vials, and stored in a desiccation cabinet until elemental and isotopic analyses.

2.6. Small volume SPE comparisons

To compare sorbents, small volume SPE isolations were performed on 20 L sub-samples of the 0.2 µm-filtered UF feed water used for the larger volume surface and deep (2500 m) samples. Glass chromatography columns were packed with 50 g of either PPL or HP-20 sorbent (Supelco Diaion® HP-20, 250–850 µm particle size, 260 Å mean pore size, Sigma-Aldrich SKU: 13,607) and experiments were conducted in parallel, with samples from the same seawater batch. Sample water was acidified to pH 2 with 40 mL of 6 N HCl in 24 L polycarbonate (PC) carboys and pumped continuously through silicon tubing to the columns at a flow rate matched to the gravity flow (drain) rate for each column (100–200 mL/min). After loading the acidified 20 L samples, the sorbent was desalted with 600 mL pH 2 ultrapure water, and retained material was eluted with six 50 mL additions of methanol and collected in pre-combusted glass bottles. Methanol samples were stored at − 20 °C, and processed to dry powders as described above.

2.7. Total DOM

Subsamples for dissolved organic carbon (DOC) and total dissolved nitrogen (TDN) concentration measurements were collected into pre-combusted 40 mL borosilicate glass vials following 0.2 µm-filtration. Samples were stored at − 20 °C until analysis. Subsamples for [DOC]

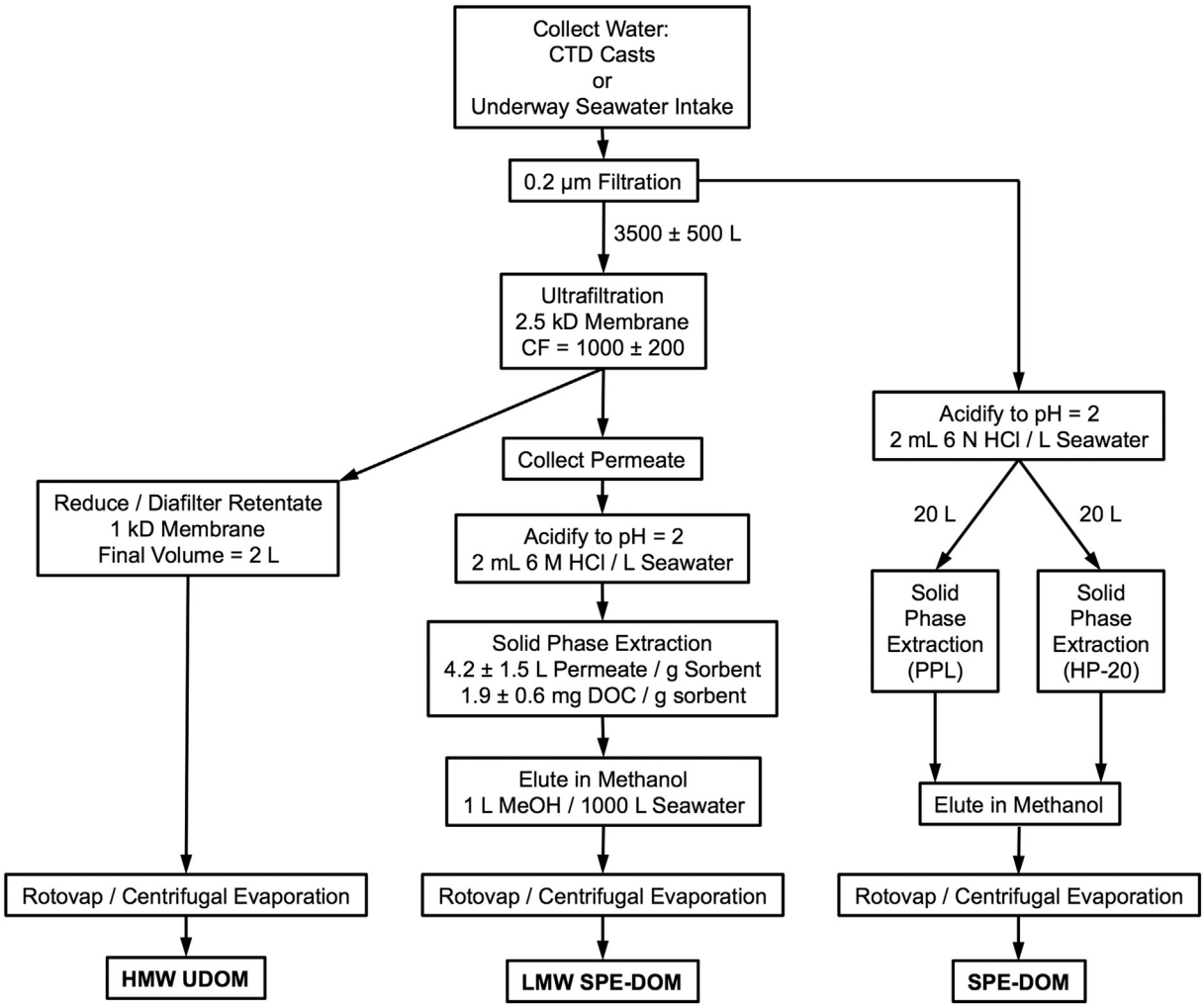

Fig. 1. Flow chart detailing the steps involved in the isolation of high molecular weight ultrafiltered dissolved organic matter (HMW UDOM), low molecular weight solid phase extracted dissolved organic matter (LMW SPE-DOM), and traditional solid phase extracted dissolved organic matter (SPE-DOM). CF: concentration factor, ratio of volume filtered to final retentate volume.

and [TDN] were also taken from the UF system permeate to evaluate mass balance. An "integrated" permeate sample (e.g., Benner et al., 1997) was prepared by sampling and combining equal volumes (100 mL) collected at constant time intervals throughout the ultrafiltration. DOC and TDN concentration measurements were made using the high temperature oxidation method with a Shimadzu TOC-V in the Carlson lab at UCSB (https://labs.eemb.ucsb.edu/carlson/craig/services). DOC concentration measurement errors represent the standard deviation of n = 3 replicate measurements. Total DON concentrations were determined by subtracting the sum of dissolved inorganic nitrogen (DIN) species (nitrate, nitrite, ammonia) from TDN. DIN concentrations were determined using a Lachat QuickChem 8000 Flow Injection Analyzer. Ammonia concentrations were below the limit of quantification (0.36 µM) for all samples using QuickChem® Method 31-107-06-1-B. Nitrate and nitrite concentrations were measured as the sum of the two analytes using QuickChem® Method 31-107-04-1-C. The limit of detection for [NO3 + NO2] using this method was 0.5 µM and the average precision of replicate standard measurements was ± 1.4 µM. In the case of [DON], measurement errors represent the propagated analytical uncertainty from the subtraction of [DIN] from [TDN]. DOC concentrations measurements were also determined via UV oxidation, cryogenic purification and manometric determination at UC Irvine. DOC concentrations were similar between the two methods and the presented values represent the error weighted mean of both measurements. For all sample depths, 0.2 µm-filtered seawater was also collected for C isotopic ($\delta^{13}C$, $\Delta^{14}C$) analysis into pre-combusted 1000 mL Amber Boston Round bottles, immediately frozen and stored at − 20 °C.

2.8. Elemental and isotopic analyses

Natural abundance radiocarbon ($\Delta^{14}C$) determinations of all isolated fractions were performed at the Lawrence Livermore National Laboratory, Center for Accelerator Mass Spectrometry (LLNL-CAMS) by AMS following standard graphitization procedures (Santos et al., 2007; Vogel et al., 1984). The $\Delta^{14}C$ signature of total seawater DOC (< 0.2 µm) was determined by UV-oxidation and AMS at the UC Irvine Keck Carbon Cycle AMS Lab (Beaupré et al., 2007; Druffel et al., 2013; Walker et al., 2016b). Results are reported as age-corrected $\Delta^{14}C$ (‰) for geochemical samples and have been corrected to the date of collection and are reported in accordance with conventions set forth by Stuiver and Polach (1977). Isotopic ^{14}C results are reported as background and $\delta^{13}C$ corrected fraction modern (Fm; Supplemental Table 1), $\Delta^{14}C$ (Table 1), and conventional radiocarbon age (ybp; Supplemental Table 1).

Stable carbon ($\delta^{13}C$) and nitrogen ($\delta^{15}N$) isotope ratios were determined via elemental analyzer isotope ratio mass spectrometry (EA-IRMS) at the University of California, Santa Cruz, Stable Isotope Laboratory (UCSC-SIL; http://emerald.ucsc.edu/~silab/). Approximately 1 mg of each dry isolated DOM sample was weighed into tin

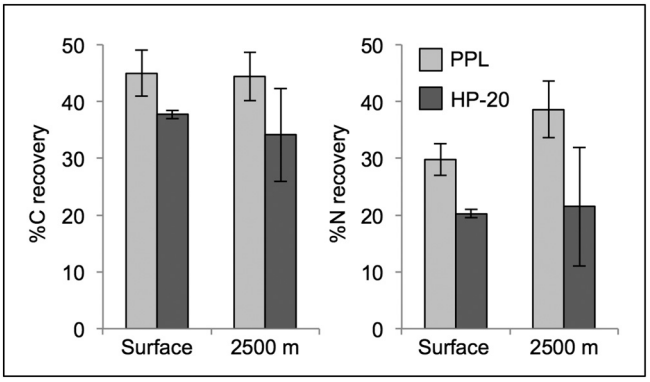

Fig. 2. Comparison of relative recovery (%) of C and N isolated by PPL (light grey) and HP-20 (dark grey) SPE sorbents. Values represent error-weighted averages of material collected on two cruises and error bars represent 1σ standard deviation of these averages.

capsules (Costec, 5 × 9 mm) for analysis. EA-IRMS analysis was conducted using a Carlo Erba CHNS-O EA1108-elemental analyzer interfaced via a ConFlo III device with a ThermoFinnigan Delta Plus XP isotope ratio mass spectrometer (Thermo Fisher Scientific). Standards, EA-IRMS protocols, and correction routines followed standard UCSC-SIL protocols. Analytical uncertainties of n = 3 replicate measurements of isotopic standards ranged from ± 0.05 to 0.1‰ for both $\delta^{13}C$ and $\delta^{15}N$. Carbon to nitrogen elemental ratios were similarly determined by elemental analysis. The presented ratios are atomic ratios $(C/N)_a$ normalized to the mass of C and N, but have been abbreviated as C/N throughout.

2.9. Data treatment and reporting of statistical uncertainty

In most cases there are no significant offsets in the measured properties of samples collected on spring and summer time cruises from the same depth, and the average values of replicate measurements were generally indistinguishable within error between cruises. In cases where there were statistically significant offsets between cruises, the differences could be interpreted as either seasonal differences or methodological variability (e.g. sample volume). In order to properly represent the potential spread of values, unless otherwise stated, all reported values represent the error-weighted average of replicate measurements (n = 3) of material collected on both summer 2014 and spring 2015 cruises. The reported standard deviation represents the variance of the weighted mean, and accounts for the uncertainty from replicate measurements and the spread of values between cruises.

3. Results and discussion

3.1. SPE sorbent comparison

To optimize our protocol for recovery of LMW DOM permeating the UF system, and to better understand potential for compositional bias, we first compare the elemental and isotopic properties of DOM isolated using two similar SPE sorbent formulations. We chose to evaluate Diaion HP-20 and Agilent PPL sorbents based on their application in recently published literature (Coppola et al., 2015; Green et al., 2014). These two sorbents have similar functional chemistry, but different bead size (250–850 μm for HP-20, 125 μm for PPL) and nearly an order of magnitude cost differential. The latter is an important consideration for any large-volume field application. Below we discuss the %DOC and %DON recoveries, C/N ratios, $\delta^{13}C$, $\delta^{15}N$, and $\Delta^{14}C$ values from replicate SPE experiments, placing them into the context of total DOM composition.

The PPL sorbent retains both more DOC and DON than HP-20. PPL recovered statistically identical proportions of DOC from both surface and deep water, representing 45 ± 4% (35 ± 2 μmolC/L) and 44 ± 4% (17 ± 1 μmolC/L) of total DOC respectively (average = 45 ± 3%) (Figs. 2, 3A). The HP-20 sorbent also has similar recoveries in the surface and at 2500 m (surface: 38 ± 1%, 30 ± 1 μmolC/L; deep: 34 ± 8%, 14 ± 5 μmolC/L; average = 35 ± 6%), but on average recovered significantly less DOC than PPL (two tailed *t*-test, DF = 5, t = 2.9, p = 0.03). As noted in the Materials and methods section, the DOM loading (ratio of sorbent mass to DOM mass) was within the ranges recommended in the literature (Dittmar et al., 2008; Li et al., 2016). The HP-20 SPE-DOC recoveries are similar to those reported by a study of surface waters at Station M (43 ± 6%, Coppola et al., 2015). Our recoveries using the PPL sorbent are similar to values reported in several different ocean regions (Weddell Sea surface to bottom, 43 ± 5%, Dittmar et al., 2008; Atlantic Ocean surface to bottom, 41 ± 3%, Hertkorn et al., 2013) and within one standard deviation of the average of currently published open-ocean values (53 ± 13%, representing data from Dittmar et al., 2008; Green et al., 2014; Hertkorn et al., 2013; Medeiros et al., 2015a; Stubbins et al., 2012). We note that the recovery efficiency of PPL from open-ocean waters is generally lower than the average recovery efficiency from fresh water, estuaries, and coastal waters (68 ± 11%, representing data from Dittmar et al., 2008; Li et al., 2016; Medeiros et al., 2015b; Osterholz et al., 2016). This is consistent with well-known differences in SPE-DOC recovery efficiency between freshwater and seawater using other types of hydrophobic sorbents (Mopper et al., 2007).

In contrast to DOC, the difference in relative recoveries of DON between sorbent types is substantially larger; with PPL recovering 10–20% more total DON than HP-20 from both surface and deep water. The HP-20 sorbent recovers on average 21 ± 7% of total DON, with little difference between surface and deep (21 ± 1% and 22 ± 10% respectively). PPL recovers far more DON (average PPL recovery = 34 ± 6%; two tailed *t*-test, DF = 5, t = 2.6, p = 0.045), with average recoveries more similar to those for DOC. The relative recovery of DON by PPL diverges between surface and deep isolations, with substantially higher %N recoveries in the deep ocean than the surface ocean (39 ± 3% vs. 30 ± 2%; two tailed *t*-test, DF = 10, t = 6.1, p < 0.01). Given the general chemical similarity of PPL and HP-20 sorbents, these differences are unexpected. While we do not have a mechanistic explanation, the higher relative recovery of N at depth by PPL suggests that the chemical properties of dissolved nitrogenous material in the deep sea make it substantially more amenable to isolation by PPL than HP-20.

The radiocarbon ($\Delta^{14}C$) values for both PPL and HP-20 isolated material suggest that DOC recovered by each sorbent approximates the average age of total DOC (Fig. 3F, Table 1). In surface waters, however, both sorbents have a small but consistent bias toward collecting older DOC material, with this effect greater for HP-20 extracted material (surface PPL SPE-DOC $\Delta^{14}C$ offset from total DOC = 23 ± 14‰, two tailed *t*-test, DF = 2, t = 2.2, p = 0.16; HP-20 SPE-DOC offset = 52 ± 14‰, two tailed *t*-test, DF = 2, t = 5.3, p = 0.03). In contrast, the $\Delta^{14}C$ of SPE-isolated material at depth is indistinguishable from total DOC $\Delta^{14}C$ for both sorbents (PPL SPE-DOC offset, 12 ± 14‰, two tailed *t*-test, DF = 2, t = 1.0, p = 0.42; HP-20 SPE-DOC offset, 7 ± 10‰, two tailed *t*-test, DF = 2, t = 1.0, p = 0.44). Similar to the recovery values, the measured $\Delta^{14}C$ of our isolated material also compares well with limited published data. Specifically, the $\Delta^{14}C$ offset between total DOC and HP-20 SPE-DOC is similar to a previous study (total DOC = − 299 ± 3‰, HP-20 SPE-DOC = − 323 ± 15‰, offset = 24 ± 15‰, (Coppola et al., 2015). Likewise, previous $\Delta^{14}C$ measurements of PPL extracted material are also similar to total DOC $\Delta^{14}C$ values (Flerus et al., 2012; Lechtenfeld et al., 2014). Together with our data, these observations indicate that despite only recovering approximately half of total DOM, these SPE sorbents generally retain a representative age fraction of DOM from the deep ocean, which closely approximates total DOM $\Delta^{14}C$.

In most cases, however, SPE isolates have significantly different

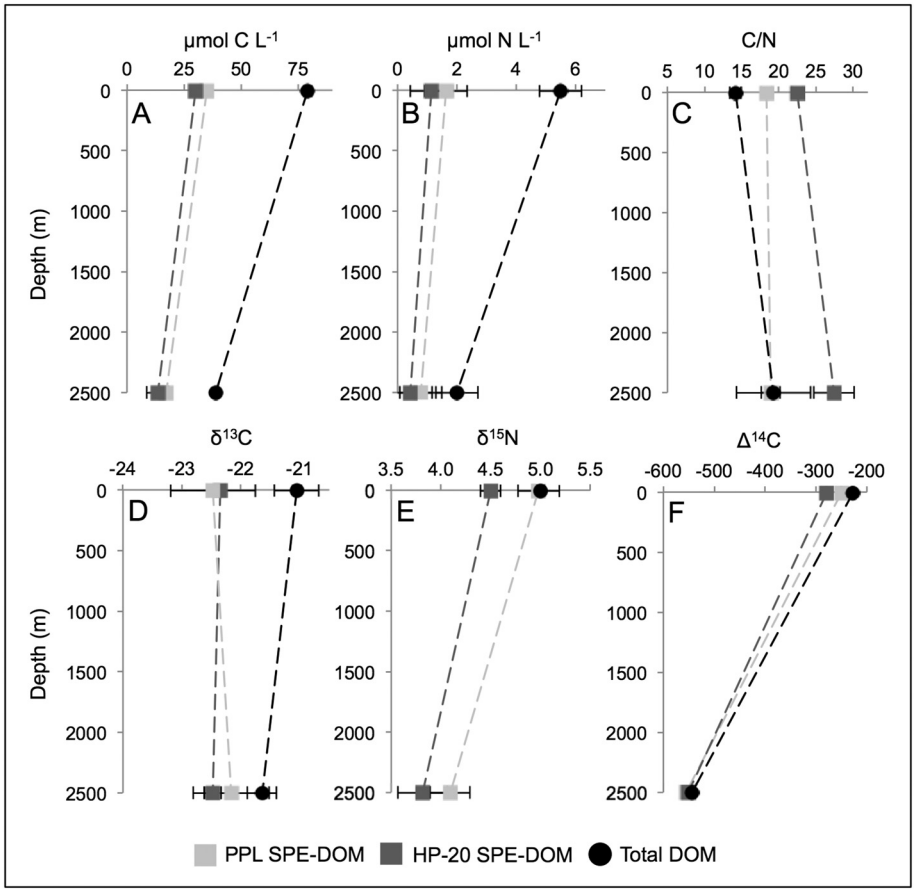

Fig. 3. Carbon and nitrogen recovery, isotopic and elemental properties of SPE-DOM isolated by PPL (light grey squares) and HP-20 (dark grey squares) compared to measurements of total seawater DOM (black circles). Values represent error weighted averages of material collected on two cruises and error bars represent 1σ standard deviation of these averages. Where no error bars are visible, SD is smaller than symbols. A) μmolC L^{-1}, B) μmolN L^{-1}, C) C/N, D) $\delta^{13}C$, E) $\delta^{15}N$, F) $\Delta^{14}C$. Total DOM $\delta^{15}N$ value from Knapp et al., 2011.

elemental and stable isotopic ratios than total DOM. The C/N ratios of SPE-DOM from the surface ocean are consistently higher than total DOM for both sorbents (Fig. 3C). However, as would be expected from DON recoveries, this difference is smaller for the PPL isolated material. For PPL SPE-DOM, the C/N values of surface samples are significantly higher than total DOM (18.4 ± 0.7 vs. 14.3 ± 0.8, two tailed *t*-test, DF = 2, t = 5.45, p = 0.03), while at depth C/N values converge, and become statistically indistinguishable (18.9 ± 1.3 vs. 19.5 ± 4.4, two tailed *t*-test, DF = 2, t = 0.18, p = 0.87). For HP-20 SPE-DOM, the offset is larger and similar in both surface and deep water (surface, 22.5 ± 0.7 vs. 14.3 ± 0.8, two tailed *t*-test, DF = 2, t = 10.9, p < 0.01; 2500 m, 27.4 ± 2.7 vs. 19.5 ± 4.4, two tailed *t*-test, DF = 2, t = 2.1, p = 0.16). We note that previously reported PPL SPE-DOM C/N ratios also show significant offsets from total DOM. For example, Green et al. (2014) report C/N ratios of 23 to 25 for PPL SPE-DOM, suggesting PPL does have a chemically selective bias against N-containing compounds. Overall, our high C/N ratios relative to total surface DOM are consistent with the low DON recoveries discussed above, as well as previous studies which measure elevated C/N ratios in SPE-DOM, and with recent work showing SPE does not efficiently isolate N-rich or high O/C ratio molecules (Chen et al., 2016; Dittmar et al., 2008; Green et al., 2014; Hertkorn et al., 2013).

SPE-DOM $\delta^{13}C$ values are lower that total DOC $\delta^{13}C$ in the surface for both sorbents. HP-20 SPE-DOC has lower $\delta^{13}C$ values than total DOC throughout the water column (surface $\delta^{13}C = -22.3 \pm 0.2$‰ vs. -21.1 ± 0.4‰, two tailed *t*-test, DF = 2, t = 3.8, p = 0.06; 2500 m $\delta^{13}C = -22.5 \pm 0.1$‰ vs. -21.6 ± 0.2‰, two tailed *t*-test, DF = 2, t = 5.7, p = 0.03). PPL SPE-DOC $\delta^{13}C$ is similarly offset in the surface (-22.5 ± 0.7‰ vs. -21.1 ± 0.4‰, two tailed *t*-test, DF = 2, t = 2.46, p = 0.13), however, PPL SPE-DOC has similar $\delta^{13}C$ values to total DOC at depth (-22.2 ± 0.6‰ vs. -21.6 ± 0.2‰, two tailed *t*-test, DF = 2, t = 1.34, p = 0.31). The low SPE-DOC $\delta^{13}C$ for both sorbents is consistent with the SPE-DOC $\Delta^{14}C$ and C/N ratio offsets mentioned above. Specifically, hydrophobic, lipid-like components of the DOM pool likely to be retained strongly by SPE sorbents are C-rich and have lower $\Delta^{14}C$ and $\delta^{13}C$ (Hwang, 2003; Loh et al., 2004; Wang et al., 2001).

Because very few studies have measured the $\delta^{15}N$ of total DON, and none have measured it in the deep ocean, a directly analogous comparison of $\delta^{15}N$ between PPL and HP-20 SPE-DON is not possible. However, comparing published $\delta^{15}N$ values of surface DON from this ocean region (5.0 ± 0.5‰, Knapp et al., 2011), we find that PPL SPE-DON $\delta^{15}N$ (5.0 ± 0.2‰) more closely approximates that of total DON than HP-20 SPE-DON $\delta^{15}N$ (4.5‰) (Fig. 3E). PPL and HP-20 SPE-DON $\delta^{15}N$ values both decrease with depth, and remain consistently offset. Again, however, without published deep total DON $\delta^{15}N$ data, it is not possible to evaluate this change relative to total DON.

Finally, we should note that it is possible that SPE sorbent blanks could contribute to these observed elemental and isotopic offsets. While we did not directly measure C blanks in this study, previous work, as well as isotope mass balance from our data indicate that this is highly unlikely as a major factor. One previous study evaluating the HP-20 sorbent for the purposes of $\Delta^{14}C$ measurements shows that no measurable carbon blank is introduced by the sorbent during processing (Coppola et al., 2015). Further, by direct measurement we find that both the PPL and HP-20 sorbent mediums used in this study have indistinguishable $\delta^{13}C$ values (27.4 ± 0.1‰), consistent with expected values for petroleum-based polymer sorbents. Based on these values, the SPE-DOC $\delta^{13}C$ offsets we observe compared to total DOC require that ~20% of our SPE-DOC be sorbent-derived blank in surface waters. This large amount of C cannot be reconciled with our relatively small $\Delta^{14}C$ offsets: a 20% contribution of sorbent C ($\Delta^{14}C = -1000$‰) in the surface would result in SPE-DOC versus total DOC $\Delta^{14}C$ offsets of 170‰ and 145‰ for PPL and HP-20 DOC respectively. The small observed

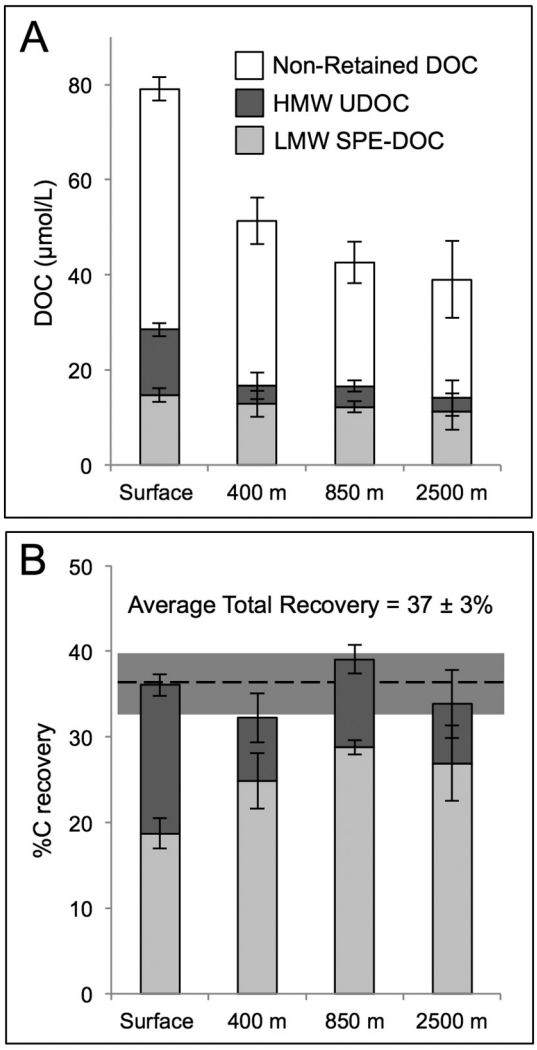

Fig. 4. Total recovery of combined UF/SPE method, indicating relative proportions of DOC pool retained by SPE and UF steps with increasing depth. A) Absolute C recoveries expressed as DOC concentration for the LMW SPE-DOC (light grey) and HMW UDOC (dark grey) isolations, compared to concentrations of non-retained DOC (white). B) relative recovery (%) of DOC by UF (dark grey) and SPE (light grey). Horizontal dotted line and grey bar represent average total recovery and SD of combined fractions. Values represent error-weighted averages of material collected on two cruises and error bars represent 1σ standard deviation of these averages.

$\Delta^{14}C$ offsets also likely exclude the possibility of significant C-contamination from residual methanol, which is similarly depleted in ^{14}C due to petroleum-derived manufacturing processes.

Overall, our SPE-DOM recovery, elemental, and isotopic composition data indicate that both PPL and HP-20 do fractionate total DOM to some degree. As is expected for a hydrophobic sorbent, both select for C-rich components, which results in the extraction of material with depleted $\delta^{13}C$ and $\Delta^{14}C$ values. For the study of DON, PPL isolates more representative material than HP-20. Where values can be compared, despite recovering only 30–40% of total DON, the $\delta^{15}N$ of PPL SPE-DOM approximates the $\delta^{15}N$ of total DON. At depth, the C/N ratio of PPL SPE-DOM is indistinguishable from total DOM C/N ratios. The consistent offsets in surface waters between SPE-DOM and total DOM suggests that some unknown fraction of younger, freshly produced DOM is not well retained by SPE. In contrast, the similarity between PPL SPE-DOM and total DOM elemental and isotopic properties at 2500 m suggests that PPL SPE-DOM is closely representative of the LMW material that dominates the deep ocean DOM reservoir. We therefore conclude that PPL represents an excellent choice for the targeted isolation of background DOM from LMW UF permeate.

3.2. Coupled UF/SPE: recovery efficiency

Given the above results, we use PPL in our combined UF/SPE approach. The UF/SPE method recovers a combined average of 37 ± 3% of total DOC, and 33 ± 7% of DON across all depths (Fig. 4). While the combined total recovery for both isolation steps is similar at all depths, there is also clear variation in the proportion of material retained by each system individually between the surface and subsurface. The UF system retains an average of 14 ± 2 µmolC/L in the surface and an average of 4 ± 1 µmolC/L from 400 m to 2500 m, representing 17 ± 1% and 9 ± 2% of total DOC respectively. SPE of the UF permeate retains a similar concentration of total DOC in the surface (15 ± 1 µmolC/L), and in the subsurface (12 ± 1 µmolC/L). As a percentage of total DOC, relative LMW SPE-DOC recovery therefore increases dramatically from surface to subsurface depths (surface average = 19 ± 2%; average of 400 m to 2500 m = 29 ± 2%).

The decrease in both the absolute and percent recovery of HMW material from surface to deep is consistent with previous observations in all ocean regions (Benner and Amon, 2015). In contrast, the absolute recovery of SPE extractable LMW DOC is similar at all depths and therefore makes up an increasing percentage of total DOC with increasing depth. This trend counteracts the decreasing recovery of HMW UDOM, resulting in an essentially identical combined recovery at all depths (37 ± 3%). The similar absolute recoveries of LMW SPE-DOM from the surface and at depth is consistent with background DOM, hypothesized to exist at similar concentrations at all ocean depths in a classical two-pool model (Carlson and Hansell, 2014; Druffel et al., 1992).

When LMW SPE-DOC recoveries are considered relative to UF permeate DOC concentrations, the recovery of LMW SPE-DOC from the surface water UF permeate is significantly lower than PPL SPE-DOC extracted from surface total DOC (27 ± 1% vs. 45 ± 4%, two tailed *t*-test, DF = 6, t = 11.7, $p < 0.01$) (Fig. 5). In contrast, at 2500 m, LMW SPE-DOC % recoveries are equivalent to PPL SPE-DOC recoveries (PPL SPE-DOC recovery = 44 ± 4%; LMW SPE-DOC recovery = 40 ± 3%; two tailed *t*-test, DF = 6, t = 1.5, p = 0.18). These differences in relative recovery between SPE-DOM and LMW SPE-DOM suggest that there is substantial overlap in the material recovered by the size-based and chemistry-based approaches. Specifically, in the surface, the UF system is removing a large portion of the material that SPE would otherwise have isolated from total DOM. At 2500 m, the difference in relative recovery of SPE-DOC and LMW SPE-DOC is not statistically significant, consistent with the substantially lower proportion of HMW material that exists in the deep ocean (Benner et al., 1997, 1992).

Put another way, these observations indicate that PPL retains both HMW (younger) and LMW (older) material, and is consistent with the $\Delta^{14}C$ data from the sorbent comparisons above. We note that published literature suggests some ocean HMW DOM may consist of aggregates of smaller molecules, bridged by inorganic cations (e.g., Chin et al., 1998; Hertkorn et al., 2006; Verdugo et al., 2004). While this could act to blur the boundaries between isolated HMW and LMW material and their respective ^{14}C ages, it should not significantly impact our overall operational isolation framework. Specifically, the concentration of HMW DOM isolated by UF is known to be dependent on ionic strength, potentially consistent with some influence of such aggregates (e.g., Walker et al., 2011), and yet UDOM is always much younger than LMW DOM (Loh et al., 2004; Santschi et al., 1995; Walker et al., 2016c, 2014, 2011). Finally, the depth related difference in the magnitude of overlap of UF and SPE isolated material also hints at chemical differences in the DOM pool, suggesting that there is a greater proportion of non-SPE isolatable DOM in the surface. This is also consistent with well-known changes in the functional character of HMW DOM with depth: specifically, while surface HMW DOM is dominated by polar biopolymers (in particular carbohydrates), deep ocean HMW DOM is dominated by carboxyl-rich aliphatic structures (CRAM) (Benner et al., 1992; Hertkorn et al., 2006; McCarthy et al., 1996).

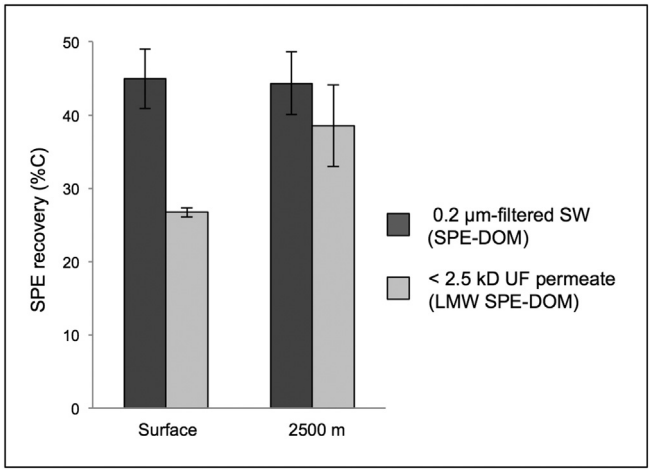

Fig. 5. Relative recovery (%) of DOC from 0.2 µm-filtered seawater (PPL SPE-DOC; dark grey) and ≤ 2.5 kD UF permeate (LMW SPE-DOC; light grey).

Finally, it may seem somewhat surprising that the combined total % recovery of the coupled UF/SPE method is lower than the recovery of SPE-DOM from whole water alone. We hypothesize that the large seawater volumes, with the associated effects of high sorbent loadings and high CFs used in these experiments (in contrast with the smaller loadings used in the sorbent comparisons), are responsible for the lower recoveries. As noted previously however, our goal here is not to maximize total recovery, but rather to isolate large amounts of DOM fractions with distinct size (HMW vs. LMW) and reactivity (^{14}C age).

3.3. Coupled UF/SPE: radiocarbon ($\Delta^{14}C$) of HMW and LMW DOM

HMW UDOC Δ^{14}C values at each depth (45 to − 375‰) are significantly different than LMW SPE-DOC Δ^{14}C values (− 350 to − 575‰) (Fig. 6). At all depths sampled in the NPSG water column, the Δ^{14}C of total DOC is intermediate between the Δ^{14}C values of the two fractions, consistent with expectations based on our operational framework. In surface waters, the offsets are large, with HMW UDOC Δ^{14}C (45 ± 10‰) significantly more positive than total DOC, and LMW SPE-DOC Δ^{14}C significantly more negative. In the deep ocean (400 m to 2500 m), LMW SPE-DOC Δ^{14}C offsets are smaller, with a constant negative Δ^{14}C offset (average offset = 37 ± 15‰) from total DOC (Supplemental Fig. 1A). In contrast, HMW UDOC Δ^{14}C values remain substantially more positive than total DOC, with a similar average Δ^{14}C offset (175 ± 15‰) at all depths.

HMW UDOM Δ^{14}C values are similar to those obtained from prior isolations of HMW UDOM in this region using similar concentration factors (Walker et al., 2011). Further, as has been observed by prior work, the ^{14}C ages of mesopelagic and deep ocean HMW UDOM (1600–3700 ybp) indicate the presence of an old DOC component. Compound class work on HMW UDOM indicates substantial diversity in the Δ^{14}C values of operationally defined biochemical fractions. While the main identifiable biochemical classes in deep UDOM appear semi-labile (as evidenced by their younger ^{14}C ages), a quantitatively smaller "lipid-like" fraction has extremely old ^{14}C ages (Loh et al., 2004). However, we note that even the oldest ^{14}C age of our bulk HMW UDOC (3700 ybp) is still significantly younger than both total DOC (6200 ybp) and LMW SPE-DOC (6800 ybp) at 2500 m.

The Δ^{14}C offsets from total DOC that we observe in both HMW UDOC and LMW SPE-DOC are consistent with previous observations about DOM size and age or reactivity (Amon and Benner, 1994; Benner and Amon, 2015; Walker et al., 2016c, 2014), and also expectations based on the relative abundance of relative size classes (Kaiser and Benner, 2009). Overall, these results indicate that this coupled method successfully isolates two separate operational fractions, dominated by either semi-labile or refractory DOM pools.

3.4. Coupled UF/SPE: elemental composition (C/N) of HMW and LMW DOM

The δ^{13}C, δ^{15}N values and C/N ratios of HMW UDOM and LMW SPE-DOM (Fig. 7, Table 1) allow a first examination of the information potential using our new isolation protocol. All bulk compositional values are dramatically different between our two fractions, reinforcing the contrasting biochemical composition of old versus young DOM pools.

The C/N ratio of LMW SPE-DOM is significantly higher (average of all depths: 26 ± 2) than HMW UDOM or total DOM, with no significant difference between surface and deep water (Surface C/N = 27.7 ± 0.4, average of 400 to 2500 m C/N = 26.1 ± 2.1; two tailed *t*-test, DF = 10, t = 1.3, p = 0.23). The elevated C/N ratios of LMW SPE-DOM suggest that older, LMW material at all depths is C-rich; consistent with highly unsaturated and aromatic structures proposed by studies using ultrahigh resolution mass spectrometry (Flerus et al., 2012; Hansman et al., 2015; Hertkorn et al., 2013; Medeiros et al., 2015a). Further, the invariant nature of LMW SPE-DOM C/N ratios with depth (Fig. 7, Table 1) is again consistent with a background pool of chemically and isotopically homogeneous DOM (Druffel et al., 1992; Druffel and Beaupré, 2009).

HMW UDOM C/N ratios are substantially lower (average of all depths: 12 ± 1), also with no significant depth structure (Surface C/N = 12.4 ± 0.5, average of 400 to 2500 m C/N = 12.3 ± 0.6; two tailed *t*-test, DF = 10, t = 0.3, p = 0.8). The HMW UDOM C/N values reported here are somewhat lower than in some past work for the Central North Pacific (e.g., 17 ± 2, Benner et al., 1997). We hypothesize that the low C/N ratios and lack of depth trend are most likely related to the high CF used, which as noted above was chosen to maximize the isolation of the highest molecular weight material with the youngest ^{14}C ages. While prior elemental data on low concentration factor UDOM shows increases in C/N ratio with depth, more consistent with the C/N ratios of the total DOM pool (Benner, 2002), a high CF UF study by Loh and co-workers also observes no significant change in HMW DOM C/N with depth from a similar ocean region (Loh et al., 2004). Therefore, the unchanging C/N ratios with depth suggest that the youngest, most labile fraction of the HMW DOM pool has a relatively uniform N-content throughout the entire Pacific water column, consistent with either non-selective degradation (McCarthy et al., 2004), or perhaps alternate surface-linked sources present at depth (Orellana and Hansell, 2012).

Surface water total DOM C/N ratios (14.1 ± 0.7) are slightly elevated compared to our HMW UDOM fraction, again consistent with expectations for our operational fractions within the two-pool model. At depth, the C/N of total DOM is substantially higher than UDOM (19 ± 5). However, because of the large errors associated with deep DON concentrations (i.e. when TDN and DIN are both high, e.g., McCarthy and Bronk, 2008), this trend is not statistically significant (two tailed *t*-test, DF = 4, t = 1.8, p = 0.15). We note that an overall increase in total DOM C/N with depth is expected based on relative proportions of HMW (low C/N) and LMW (high C/N) DOM in surface versus deep water. Overall, these HMW UDOM and LMW SPE-DOM C/N ratio offsets fit well within recent observations of broader trends between organic matter size, age, and elemental composition (Walker et al., 2016c, 2016a).

3.5. Coupled UF/SPE: stable isotopic composition ($\delta^{13}C$, $\delta^{15}N$) of HMW and LMW DOM

In the surface, the δ^{13}C value of HMW UDOC and LMW SPE-DOC fractions are statistically indistinguishable (− 22.5 ± 0.3‰ and − 22.7 ± 0.2‰ respectively; two tailed *t*-test, DF = 10, t = 1.4,

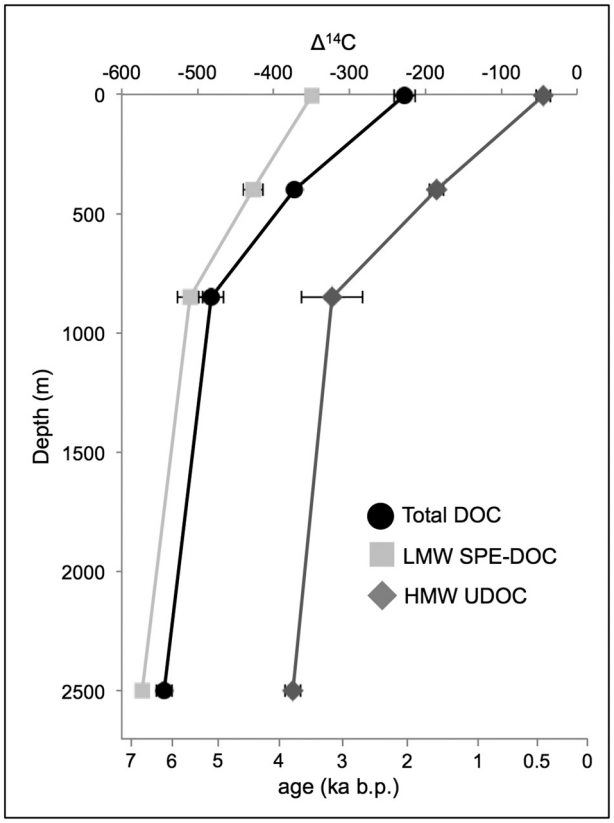

Fig. 6. $\Delta^{14}C$ of total DOC (black circles) compared to LMW SPE-DOC (light grey squares) and HMW UDOC (dark grey diamonds). Bottom axis denotes the ^{14}C age in ka. Values represent error-weighted averages of material collected on two cruises and error bars represent 1σ standard deviation of these averages.

p = 0.2) (Fig. 7). Both values however, are lower than total DOC $\delta^{13}C$ (− 21.1 ± 0.4‰). In the subsurface, the average $\delta^{13}C$ values of each fraction are offset from both each other and total DOM. There is no depth trend below 400 m in $\delta^{13}C$ within either fraction, leading to a constant offset between the two fractions (Supplemental Fig. 2C). The $\delta^{13}C$ values of LMW SPE-DOM from ≥ 400 m are always lowest (average of 400 to 2500 m: − 22.6 ± 0.4‰), the HMW UDOM always highest (average of 400 to 2500 m: − 21.4 ± 0.4‰), and the total DOM values are intermediate between the two fractions (average: − 22.1 ± 0.4‰).

The $\delta^{13}C$ results in the subsurface NPSG are consistent with expectations based on the relative functional composition of HMW and LMW pools. Specifically, LMW SPE-DOM likely contains more lipid-like and CRAM like structures (Hertkorn et al., 2006; Koprivnjak et al., 2009), consistent with both higher C/N and lower $\delta^{13}C$ values (e.g., Hayes, 2001). In contrast, the more abundant proteinaceous and carbohydrate compound classes in HMW UDOC are consistent with both lower C/N and higher $\delta^{13}C$ (Hayes, 2001). The intermediate $\delta^{13}C$ values of total DOC between LMW SPE-DOC and HMW UDOC for all depths (with the exception of the surface), further supports the conclusion that our method selectively isolates two operationally distinct fractions from different reactivity pools.

However, the large offset of both HMW UDOC and LMW SPE-DOC $\delta^{13}C$ from total DOC $\delta^{13}C$ in the surface (Fig. 7, Supplemental Fig. 1) does not seem consistent with these ideas. This result could be linked to material not retained by either UF or SPE isolations. This would require the non-retained material to have similar $\delta^{13}C$ values to total DOC (average $\delta^{13}C$ value of approximately − 20.8, by mass balance), and be composed of nominally low MW material (i.e., passes the UF membrane) that is also relatively polar (so as not to be retained by the hydrophobic sorbent). In addition, the average C/N value of the non-retained material (by mass balance) is ~14, and therefore not consistent with expectations for ^{13}C-enriched proteinaceous material. Finally, the presence of this offset only in the surface samples, repeated in both seasonal cruises, suggests this non-retained DOM is fresh, labile, and disappears rapidly with degradation. However, this would seem to conflict with the average value for mass balance derived $\Delta^{14}C$ for the non-retained material (− 240‰). An alternate explanation therefore, is that rather than missing material having an elevated $\delta^{13}C$, the HMW material isolated in the surface is skewed toward lower $\delta^{13}C$ values by the presence of a ^{13}C deplete component.

The $\delta^{15}N$ values of LMW SPE-DON (average of all depths: 3.5 ± 0.3‰) and HMW UDON (average of all depths: 6.6 ± 0.4‰) are significantly different throughout the water column (two tailed *t*-test, DF = 22, t = 21.4, p < 0.01) (Fig. 7). LMW SPE-DON $\delta^{15}N$ is significantly lower than HMW UDON $\delta^{15}N$ at all depths, with an increasing offset from surface to deep. Average surface LMW SPE-DON $\delta^{15}N$ is 4.0 ± 0.3‰, and decreases to a constant value in subsurface samples (average of all subsurface samples: 3.4 ± 0.1‰). HMW UDON $\delta^{15}N$ has the opposite behavior with depth: surface values average 6.3 ± 0.3‰, with higher average subsurface values of 6.7 ± 0.3‰. While the offset between HMW UDON and LMW SPE-DON $\delta^{15}N$ values are significant at all depths (average offset over entire water column = 3.1 ± 0.6‰), the offset also increases with increasing depth (Supplemental Fig. 2D, surface offset = 2.2 ± 0.4‰, 2500 m offset = 3.4 ± 0.3‰, two tailed *t*-test, DF = 4, t = 4.1, p = 0.01).

Published values for bulk DON $\delta^{15}N$ in surface water for this region

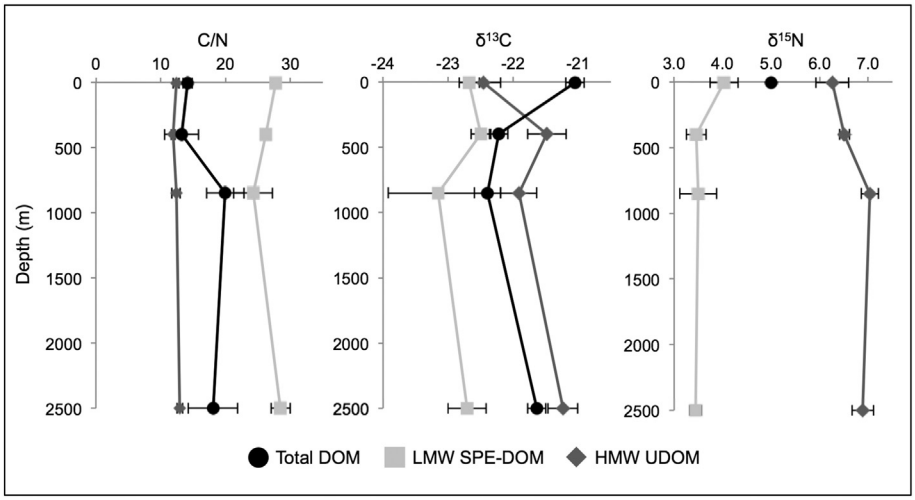

Fig. 7. Depth profiles of elemental ratio (C/N), $\delta^{13}C$, and $\delta^{15}N$ values of total DOM (black circles) compared to LMW SPE-DOM (light grey squares) and HMW UDOM (dark grey diamonds). Values represent error-weighted averages of material collected on two cruises and error bars represent 1σ standard deviation of these averages. Total DOM $\delta^{15}N$ value from Knapp et al., 2011.

Table 1

Sample Type	Depth	DOC	±	DON	±	% Recovery		(C/N)a	±	δ15N	±	δ13C	±	Δ14C	±
	(m)	(μmol/L)		(μmol/L)		(%C)	(%N)			(‰)		(‰)		(‰)	
Total DOC	7.5	79.8	0.6	5.7	0.6	–	–	14.1	0.9	–	–	− 20.8	0.2	− 215.1	2.6
Total DOC	7.5	75.9	1.2	5.3	0.7	–	–	14.3	1.4	–	–	− 21.3	0.2	− 234.5	1.9
Total DOC	400	47.2	2.8	3.6	0.4	–	–	13.2	2.8	–	–	− 22.7	0.2	− 370.6	2.3
Total DOC	400	45.5	7.8	3.5	0.8	–	–	13.1	7.9	–	–	− 21.7	0.2	− 374.1	1.7
Total DOC	850	41.0	1.1	2.1	0.5	–	–	19.7	1.2	–	–	− 22.4	0.2	− 466.7	2.6
Total DOC	850	41.8	4.6	1.8	0.4	–	–	23.4	4.6	–	–	–	–	− 490.0	1.8
Total DOC	2500	34.8	5.3	2.0	0.4	–	–	17.8	5.3	–	–	− 21.8	0.2	− 537.4	2.0
Total DOC	2500	38.6	5.3	2.1	0.5	–	–	18.4	5.3	–	–	− 21.5	0.2	− 551.6	2.2
PPL SPE-DOM	7.5	33.7	–	1.6	–	42.1	27.8	18.3	0.2	5.1	0.2	− 23.0	0.08	− 248.0	2.1
PPL SPE-DOM	7.5	36.3	–	1.7	–	47.8	31.7	18.4	0.13	4.8	0.2	− 22.0	0.08	− 253.0	2.7
PPL SPE-DOM	2500	17.5	–	0.8	–	41.4	42.1	18.2	0.2	4.0	0.2	− 22.6	0.08	− 549.1	1.5
PPL SPE-DOM	2500	16.9	–	0.7	–	47.3	35.1	19.6	0.13	4.2	0.2	− 21.7	0.08	− 561.8	2.0
HP-20 SPE-DOM	7.5	30.1	–	1.1	–	37.7	20.2	22.5	0.2	4.5	0.2	− 22.3	0.08	− 279.6	2.2
HP-20 SPE-DOM	2500	16.9	–	0.6	–	39.9	28.9	25.6	0.2	4.0	0.2	− 22.4	0.08	− 551.6	2.0
HP-20 SPE-DOM	2500	10.1	–	0.3	–	28.3	14.1	29.3	0.13	3.7	0.2	− 22.6	0.08	− 550.4	1.7
HMW UDOM	7.5	14.2	–	1.1	–	17.8	19.5	12.9	0.06	6.2	0.1	− 22.1	0.05	− 37.3	3.8
HMW UDOM	7.5	12.4	–	0.9	–	16.3	16.2	12.3	0.02	6.7	0.3	− 22.5	0.01	− 50.0	3.3
HMW UDOM	400	3.7	–	0.3	–	7.8	8.9	11.9	0.06	6.5	0.1	− 21.5	0.01	− 190.4	2.2
HMW UDOM	400	4.8	–	0.4	–	10.6	10.4	11.5	0.2	6.6	0.1	− 21.9	0.3	− 177.3	2.9
HMW UDOM	850	4.4	–	0.3	–	10.7	16.7	13.1	0.03	6.8	0.1	− 21.9	0.05	− 343.7	2.1
HMW UDOM	850	3.9	–	0.3	–	9.2	15.2	12.2	0.02	7.1	0.1	− 21.5	0.3	− 286.9	2.8
HMW UDOM	2500	3.3	–	0.3	–	9.5	13.9	13.1	0.1	6.8	0.2	− 21.1	0.04	− 379.7	1.8
HMW UDOM	2500	2.5	–	0.2	–	6.4	8.1	12.5	0.1	7.0	0.3	− 21.5	0.06	− 365.7	2.3
LMW SPE-DOM	7.5	14.5	–	0.4	–	18.1	7.8	28.2	0.3	3.6	0.07	− 22.9	0.06	− 354.8	2.1
LMW SPE-DOM	7.5	15.5	–	0.5	–	20.4	9.0	27.6	0.1	4.0	0.01	− 22.6	0.03	− 343.0	2.3
LMW SPE-DOM	400	12.9	–	0.4	–	25.2	11.8	26.2	0.1	3.4	0.2	− 22.5	0.01	− 420.4	1.7
LMW SPE-DOM	400	12.5	–	0.4	–	22.5	11.8	26.1	1.9	3.6	0.4	− 22.7	0.4	− 438.8	2.2
LMW SPE-DOM	850	12.2	–	0.4	–	28.8	20.8	24.2	0.0	3.6	0.1	− 22.2	0.04	− 518.0	1.5
LMW SPE-DOM	850	5.5	–	0.2	–	12.4	9.3	28.4	0.1	3.1	0.2	− 23.3	0.02	− 494.3	2.1
LMW SPE-DOM	2500	10.7	–	0.3	–	25.3	17.7	26.4	0.2	3.5	0.2	− 22.4	0.1	− 569.7	1.4
LMW SPE-DOM	2500	11.7	–	0.4	–	28.5	16.7	28.5	0.03	3.4	0.2	− 22.8	0.06	− 577.6	1.7

* Total DOC values were measured at UCI Keck Carbon Cycle AMS Lab.

(5.0 ± 0.5‰, Knapp et al., 2011) are intermediate between the two isolated fractions (Fig. 7, Table 1). In addition, the general direction of the offset with depth (i.e., HMW DON having higher $\delta^{15}N$ values than LMW DON) is also consistent with the few prior observations in oligotrophic surface waters (Knapp et al., 2012). These novel data raise new questions regarding N-sources, and in particular what cycling processes over multi-centennial to millennial ocean mixing timescales could result in a similar $\delta^{15}N$ pattern at all depths in the North Central Pacific. While more detailed work will be required to address these questions, the difference in $\delta^{15}N$ value between our operational fractions in particular underscores the new potential of this approach to isolate separate DOM fractions with novel properties and distinct composition.

3.6. SPE-DOM vs. LMW SPE-DOM

As discussed in the Coupled UF/SPE: recovery efficiency section, recovery data indicates that there is substantial overlap in the material collected by UF and SPE. This is further supported by the differences in the elemental and isotopic properties of SPE-DOM compared to LMW SPE-DOM (Supplemental Fig. 3). Whereas PPL SPE-DOM properties approximate total DOM in numerous cases (especially in the deep ocean), the properties of LMW SPE-DOM are consistently different than total DOC. LMW SPE-DOM is older, has higher C/N ratios, and lower $\delta^{13}C$ and $\delta^{15}N$ values that both SPE-DOM and total DOM at all depths. This suggests that there is some younger, lower C/N, higher $\delta^{13}C$ and $\delta^{15}N$ material which is isolated by SPE, but is not isolated in the LMW SPE-DOM fraction because of prior removal by UF. The offset is greatest in the surface where there is the highest concentration of HMW DOM, further suggesting that the offsets are the result of partial collection of HMW DOM by SPE. Overall, this demonstrates that the removal of HMW DOM by UF is required for the subsequent targeted isolation of refractory DOM via SPE.

4. Summary and conclusions

We describe a new approach that targets the isolation of operational DOM fractions with strongly contrasting average age, molecular size, and bulk composition. We couple UF with SPE isolation from the UF permeate to selectively isolate HMW and LMW DOM respectively. The composition of the HMW UDOM samples is consistent with younger, more N-rich, semi-labile DOM, while the composition of LMW SPE-DOM isolates is consistent with older, C-rich, more refractory DOM. The contrasting properties of the individual isolates from surface to deep NPSG waters confirm that our MW partition is effective at isolating material with strongly distinct properties. Further, our large volume isolation protocol allows gram quantities of these DOM fractions to be isolated for subsequent analysis. The scalability of this approach further enables a wide range of detailed analyses, such as compound-specific stable or radio isotopic analyses, for which sample limitation can otherwise prohibit.

In order to optimize our coupled UF/SPE method, we performed a comprehensive set of tests with two SPE sorbents commonly applied in recent literature for DOM isolation; comparing the elemental ratios, stable isotope ratios, and radiocarbon age of SPE-DOM with the same properties in total DOM. These tests showed that PPL generally performs better than HP-20, with higher overall DOC recoveries and with elemental and isotopic compositions more representative of total DOM, especially in the deep ocean. However, our data also suggests that the chemical and isotopic composition of SPE-DOM, in particular for nitrogenous organic material, is strongly depth-dependent. SPE of surface DOM discriminates strongly against organic nitrogen, and has $\Delta^{14}C$ and $\delta^{13}C$ values offset from total DOC, consistent with preferential isolation of hydrophobic, C-rich DOM. In contrast, PPL SPE-DOM in deep NPSG waters is statistically indistinguishable from total DOM for all elemental and isotopic properties we measure, including C/N ratios. This suggests

that PPL is well suited to the study of the refractory, background DOM pool. However, it is also clear from isotopic and recovery efficiency data that PPL SPE-DOM isolates from any depth contain a mixture of both older, refractory DOM and a younger, semi-labile component. Therefore, the removal of the HMW young, semi-labile material by UF prior to SPE is required in order to isolate an older, more refractory component and limit the confounding influences of reactivity mixtures.

Together, our results underscore the compositional and isotopic heterogeneity of marine DOM and highlight the inherent problems with attempting to isolate truly representative DOM samples. We suggest that targeted isolation approaches, which exploit differences in DOM composition, can yield samples that allow more specific testing of multiple current hypotheses regarding the origin and composition of excess, semi-labile DOM and background, refractory DOM. The current era of DOM research is an exciting one, with multiple ideas suggested to explain refractory DOM persistence and biogeochemical cycling. Molecular diversity, dilution, microbial degradation, molecular size and composition, photo-oxidation, and micro-gel aggregation have all been suggested as key controls on refractory DOM formation (Arrieta et al., 2015; Chin et al., 1998; Dittmar, 2014; Flerus et al., 2012; Jiao et al., 2010; Lechtenfeld et al., 2014; Walker et al., 2016a). This isolation approach represents a new tool for directly evaluating the composition of distinct DOM reactivity pools, and allows for testing new hypotheses regarding DOM cycling in the ocean.

Supplementary data to this article can be found online at http://dx.doi.org/10.1016/j.marchem.2017.06.007.

Acknowledgements

The authors would foremost like to thank the captains and crew of the R/V Kilo Moana. Additional thanks to Amy Bour, Jessie Zupcic-Moore, Danielle Glynn, and Yasu Yamaguchi for assistance with sample collection and processing, Colin Carney and Dyke Andreasen of UCSC-SIL for assisting with EA-IRMS analysis, and Alexandra Hedgpeth and Paula Zermeno of LLNL-CAMS for assistance with AMS sample preparation. This work was primarily supported by a grant from NSF Chemical Oceanography (Award # 1358041). Total DOC ^{14}C analysis was performed under a UCI Keck Carbon Cycle AMS Lab postdoctoral scholarship to B.D.W. A portion of this work was performed at the US DOE Lawrence Livermore National Laboratory under contract DE-AC52-07NA27344.

References

Aluwihare, L.I., Repeta, D.J., Chen, R.F., 1997. A major biopolymeric component to dissolved organic carbon in surface sea water. Nature 387, 166–169. http://dx.doi.org/10.1038/387166a0.

Amador, J.A., Milne, P.J., Moore, C.A., Zika, R.G., 1990. Extraction of chromophoric humic substances from seawater. Mar. Chem. 29, 1–17. http://dx.doi.org/10.1016/0304-4203(90)90002-t.

Amon, R.M.W., Benner, R., 1994. Rapid cycling of high-molecular-weight dissolved organic matter in the ocean. Nature 369, 549–552. http://dx.doi.org/10.1038/369549a0.

Amon, R.M.W., Benner, R., 1996. Bacterial utilization of different size classes of dissolved organic matter. Limnol. Oceanogr. 41, 41–51. http://dx.doi.org/10.4319/lo.1996.41.1.0041.

Arrieta, J.M., Mayol, E., Hansman, R.L., Herndl, G.J., Dittmar, T., Duarte, C.M., 2015. Dilution limits dissolved organic carbon utilization in the deep ocean. Science 348, 331–333. http://dx.doi.org/10.1126/science.1258955.

Beaupré, S.R., Aluwihare, L.I., 2010. Constraining the 2-component model of marine dissolved organic radiocarbon. Deep-Sea Res. II Top. Stud. Oceanogr. 57 (16), 1494–1503. http://dx.doi.org/10.1016/j.dsr2.2010.02.017.

Beaupré, S.R., Druffel, E.R.M., Griffin, S., 2007. A low-blank photochemical extraction system for concentration and isotopic analyses of marine dissolved organic carbon. Limnol. Oceanogr. Methods 5, 174–184. http://dx.doi.org/10.4319/lom.2007.5.174.

Benner, R., 2002. Chemical Composition and Reactivity. In: Hansel, D.A., Carlson, C.A. (Eds.), The Biogeochemistry of Marine Dissolved Organic Matter. Academic Press, pp. 59–87.

Benner, R., Amon, R.M.W., 2015. The size-reactivity continuum of major bioelements in the ocean. Annu. Rev. Mar. Sci. 7, 185–205. http://dx.doi.org/10.1146/annurev-marine-010213-135126.

Benner, R., Pakulski, J.D., McCarthy, M.D., Hedges, J.I., Hatcher, P.G., 1992. Bulk chemical characteristics of dissolved organic matter in the ocean. Science 255, 1561–1564.

Benner, R., Biddanda, B., Black, B., McCarthy, M.D., 1997. Abundance, size distribution, and stable carbon and nitrogen isotopic compositions of marine organic matter isolated by tangential-flow ultrafiltration. Mar. Chem. 57, 243–263.

Carlson, C.A., Hansell, D.A., 2014. DOM Sources, Sinks, Reactivity, and Budgets. In: Hansel, D.A., Carlson, C.A. (Eds.), The Biogeochemistry of Marine Dissolved Organic Matter. Academic Press, pp. 65–126.

Chen, M., Kim, S., Park, J.E., Jung, H.J., Hur, J., 2016. Structural and compositional changes of dissolved organic matter upon solid-phase extraction tracked by multiple analytical tools. Anal. Bioanal. Chem. 408, 6249–6258. http://dx.doi.org/10.1007/s00216-016-9728-0.

Chin, W.C., Orellana, M.V., Verdugo, P., 1998. Spontaneous assembly of marine dissolved organic matter into polymer gels. Nature 391, 568–572. http://dx.doi.org/10.1038/35345.

Coppola, A.I., Walker, B.D., Druffel, E.R.M., 2015. Solid phase extraction method for the study of black carbon cycling in dissolved organic carbon using radiocarbon. Mar. Chem. 177, 697–705. http://dx.doi.org/10.1016/j.marchem.2015.10.010.

Dittmar, T., 2014. Reasons behind the long-term stability of dissolved organic matter. In: Hansel, D.A., Carlson, C.A. (Eds.), Biogeochemistry of Marine Dissolved Organic Matter. Academic Press, pp. 369–388.

Dittmar, T., Stubbins, A., 2014. Dissolved organic matter in aquatic systems. In: Treatise on Geochemistry. Elsevier, pp. 125–156. http://dx.doi.org/10.1016/B978-0-08-095975-7.01010-X.

Dittmar, T., Koch, B., Hertkorn, N., Kattner, G., 2008. A simple and efficient method for the solid-phase extraction of dissolved organic matter (SPE-DOM) from seawater. Limnol. Oceanogr. Methods 6, 230–235.

Druffel, E.R.M., Beaupré, S.R., 2009. Constraining the propagation of bomb-radiocarbon through the dissolved organic carbon (DOC) pool in the northeast Pacific Ocean. Deep-Sea Res. I Oceanogr. Res. Pap. 56, 1717–1726. http://dx.doi.org/10.1016/j.dsr.2009.05.008.

Druffel, E., Williams, P.M., Bauer, J.E., Ertel, J.R., 1992. Cycling of dissolved and particulate organic-matter in the open ocean. J. Geophys. Res. 97, 15639–15659.

Druffel, E.R.M., Griffin, S., Walker, B.D., Coppola, A.I., Glynn, D.S., 2013. Total uncertainty of radiocarbon measurements of marine dissolved organic carbon and methodological recommendations. Radiocarbon 55, 1135–1141.

Flerus, R., Lechtenfeld, O.J., Koch, B.P., McCallister, S.L., Schmitt-Kopplin, P., Benner, R., Kaiser, K., Kattner, G., 2012. A molecular perspective on the ageing of marine dissolved organic matter. Biogeosciences 9, 1935–1955. http://dx.doi.org/10.5194/bg-9-1935-2012.

Green, S.A., Blough, N.V., 1994. Optical absorption and fluorescence properties of chromophoric dissolved organic matter in natural waters. Limnol. Oceanogr. 39, 1903–1916. http://dx.doi.org/10.4319/lo.1994.39.8.1903.

Green, N.W., Perdue, E.M., Aiken, G.R., Butler, K.D., Chen, H., Dittmar, T., Niggemann, J., Stubbins, A., 2014. An intercomparison of three methods for the large-scale isolation of oceanic dissolved organic matter. Mar. Chem. 161, 14–19. http://dx.doi.org/10.1016/j.marchem.2014.01.012.

Guo, L., Santschi, P.H., Cifuentes, L.A., Trumbore, S.E., Southon, J., 1996. Cycling of high-molecular-weight dissolved organic matter in the Middle Atlantic Bight as revealed by carbon isotopic (13C and 14C) signatures. Limnol. Oceanogr. 41, 1242–1252. http://dx.doi.org/10.4319/lo.1996.41.6.1242.

Hansman, R.L., Dittmar, T., Herndl, G.J., 2015. Conservation of dissolved organic matter molecular composition during mixing of the deep water masses of the northeast Atlantic Ocean. Mar. Chem. 177, 288–297. http://dx.doi.org/10.1016/j.marchem.2015.06.001.

Hayes, J.M., 2001. Fractionation of carbon and hydrogen isotopes in biosynthetic processes. Rev. Mineral. Geochem. 43, 225–277. http://dx.doi.org/10.2138/gsrmg.43.1.225.

Hertkorn, N., Benner, R., Frommberger, M., Schmitt-Kopplin, P., Witt, M., Kaiser, K., Kettrup, A., Hedges, J.I., 2006. Characterization of a major refractory component of marine dissolved organic matter. Geochim. Cosmochim. Acta 70, 2990–3010. http://dx.doi.org/10.1016/j.gca.2006.03.021.

Hertkorn, N., Harir, M., Koch, B.P., Michalke, B., Schmitt-Kopplin, P., 2013. High-field NMR spectroscopy and FTICR mass spectrometry: powerful discovery tools for the molecular level characterization of marine dissolved organic matter. Biogeosciences 10, 1583–1624. http://dx.doi.org/10.5194/bg-10-1583-2013.

Hwang, J., 2003. Lipid-like material as the source of the uncharacterized organic carbon in the ocean? Science 299, 881–884. http://dx.doi.org/10.1126/science.1078508.

Jiao, N., Herndl, G.J., Hansell, D.A., Benner, R., Kattner, G., Wilhelm, S.W., Kirchman, D.L., Weinbauer, M.G., Luo, T., Chen, F., Azam, F., 2010. Microbial production of recalcitrant dissolved organic matter: long-term carbon storage in the global ocean. Nat. Publ. Group 8, 593–599. http://dx.doi.org/10.1038/nrmicro2386.

Kaiser, K., Benner, R., 2009. Biochemical composition and size distribution of organic matter at the Pacific and Atlantic time-series stations. Mar. Chem. 113, 63–77. http://dx.doi.org/10.1016/j.marchem.2008.12.004.

Kilduff, J., Weber Jr., W.J., 1992. Transport and separation of organic macromolecules in ultrafiltration processes. Environ. Sci. Technol. 26, 569–577. http://dx.doi.org/10.1021/es00027a021.

Knapp, A.N., Sigman, D.M., Lipschultz, F., Kustka, A.B., Capone, D.G., 2011. Interbasin isotopic correspondence between upper-ocean bulk DON and subsurface nitrate and its implications for marine nitrogen cycling. Glob. Biogeochem. Cycles 25, GB4004. http://dx.doi.org/10.1029/2010GB003878.

Knapp, A.N., Sigman, D.M., Kustka, A.B., Sañudo-Wilhelmy, S.A., Capone, D.G., 2012. The distinct nitrogen isotopic compositions of low and high molecular weight marine DON. Mar. Chem. 136–137, 24–33. http://dx.doi.org/10.1016/j.marchem.2012.05.001.

Koprivnjak, J.F., Pfromm, P.H., Ingall, E., Vetter, T.A., Schmitt-Kopplin, P., Hertkorn, N., Frommberger, M., Knicker, H., Perdue, E.M., 2009. Chemical and spectroscopic characterization of marine dissolved organic matter isolated using coupled reverse osmosis–electrodialysis. Geochim. Cosmochim. Acta 73, 4215–4231. http://dx.doi.org/10.1016/j.gca.2009.04.010.

Lechtenfeld, O.J., Kattner, G., Flerus, R., 2014. Molecular transformation and degradation of refractory dissolved organic matter in the Atlantic and Southern Ocean. Geochim. Cosmochim. Acta 126, 321–337. http://dx.doi.org/10.1016/j.gca.2013.11.009.

Li, Y., Harir, M., Lucio, M., Kanawati, B., Smirnov, K., Flerus, R., Koch, B.P., Schmitt-Kopplin, P., Hertkorn, N., 2016. Proposed guidelines for solid phase extraction of Suwannee River dissolved organic matter. Anal. Chem. 88, 6680–6688. http://dx.doi.org/10.1021/acs.analchem.5b04501.

Loh, A.N., Bauer, J.E., Druffel, E.R.M., 2004. Variable ageing and storage of dissolved organic components in the open ocean. Nature 430, 877–881. http://dx.doi.org/10.1038/nature02780.

McCarthy, M.D., Bronk, D.A., 2008. Analytical methods for the study of nitrogen. In: Capone, D.G., Bronk, D.A., Mulholland, M.R., Carpenter, E.J. (Eds.), Nitrogen in the Marine Environment. Elsevier, pp. 1219–1275.

McCarthy, M., Hedges, J., Benner, R., 1996. Major biochemical composition of dissolved high molecular weight organic matter in seawater. Mar. Chem. 55, 281–297.

McCarthy, M.D., Benner, R., Lee, C., Hedges, J.I., Fogel, M.L., 2004. Amino acid carbon isotopic fractionation patterns in oceanic dissolved organic matter: an unaltered photoautotrophic source for dissolved organic nitrogen in the ocean? Mar. Chem. 92 (1–4), 123–134. http://dx.doi.org/10.1016/j.marchem.2004.06.021.

Medeiros, P.M., Seidel, M., Powers, L.C., Dittmar, T., Hansell, D.A., Miller, W.L., 2015a. Dissolved organic matter composition and photochemical transformations in the northern North Pacific Ocean. Geophys. Res. Lett. 42, 863–870. http://dx.doi.org/10.1002/2014GL062663.

Medeiros, P.M., Seidel, M., Ward, N.D., Carpenter, E.J., Gomes, H.R., Niggemann, J., Krusche, A.V., Richey, J.E., Yager, P.L., Dittmar, T., 2015b. Fate of the Amazon River dissolved organic matter in the tropical Atlantic Ocean. Glob. Biogeochem. Cycles 29, 677–690. http://dx.doi.org/10.1002/2015GB005115.

Mopper, K., Stubbins, A., Ritchie, J.D., Bialk, H.M., Hatcher, P.G., 2007. Advanced instrumental approaches for characterization of marine dissolved organic matter: extraction techniques, mass spectrometry, and nuclear magnetic resonance spectroscopy. Chem. Rev. 107, 419–442. http://dx.doi.org/10.1021/cr050359b.

Mortazavi, B., Chanton, J.P., 2004. Use of Keeling plots to determine sources of dissolved organic carbon in nearshore and open ocean systems. Limnol. Oceanogr. 49, 102–108.

Orellana, M.V., Hansell, D.A., 2012. Ribulose-1,5-bisphosphate carboxylase/oxygenase (RuBisCO): a long-lived protein in the deep ocean. Limnol. Oceanogr. 57, 826–834. http://dx.doi.org/10.4319/lo.2012.57.3.0826.

Osterholz, H., Kirchman, D.L., Niggemann, J., Dittmar, T., 2016. Environmental drivers of dissolved organic matter molecular composition in the Delaware Estuary. Front. Earth Sci. 4, 231. http://dx.doi.org/10.3389/feart.2016.00095.

Roland, L.A., McCarthy, M.D., Peterson, T.D., Walker, B.D., 2009. A large-volume microfiltration system for isolating suspended particulate organic matter: fabrication and assessment versus GFF filters in central North Pacific. Limnol. Oceanogr. Methods 7, 64–80.

Santos, G.M., Southon, J.R., Griffin, S., Beaupré, S.R., Druffel, E.R.M., 2007. Ultra small-mass AMS 14C sample preparation and analyses at KCCAMS/UCI Facility. Nucl. Instrum. Meth. Phys. Res. Section B: Beam Interactions Mater. Atoms 259, 293–302. http://dx.doi.org/10.1016/j.nimb.2007.01.172.

Santschi, P.H., Guo, L., Baskaran, M., Trumbore, S., Southon, J., Bianchi, T.S., Honeyman, B., Cifuentes, L., 1995. Isotopic evidence for the contemporary origin of high-molecular weight organic matter in oceanic environments. Geochim. Cosmochim. Acta 59, 625–631. http://dx.doi.org/10.1016/0016-7037(94)00378-Y.

Schwede-Thomas, S.B., Chin, Y.P., Dria, K.J., Hatcher, P., Kaiser, E., Sulzberger, B., 2005. Characterizing the properties of dissolved organic matter isolated by XAD and C-18 solid phase extraction and ultrafiltration. Aquat. Sci. 67, 61–71. http://dx.doi.org/10.1007/s00027-004-0735-4.

Simjouw, J.-P., Minor, E.C., Mopper, K., 2005. Isolation and characterization of estuarine dissolved organic matter: comparison of ultrafiltration and C18 solid-phase extraction techniques. Mar. Chem. 96, 219–235. http://dx.doi.org/10.1016/j.marchem.2005.01.003.

Stubbins, A., Niggemann, J., Dittmar, T., 2012. Photo-lability of deep ocean dissolved black carbon. Biogeosciences 9, 1661–1670. http://dx.doi.org/10.5194/bg-9-1661-2012.

Stuiver, M., Polach, H.A., 1977. Discussion: Reporting of 14C Data. Radiocarbon 19 (3), 355–363. http://dx.doi.org/10.1017/s0033822200003672.

Town, R.M., Powell, H., 1993. Limitations of XAD resins for the isolation of the non-colloidal humic fraction in soil extracts and aquatic samples. Anal. Chim. Acta 271, 195–202.

Verdugo, P., Alldredge, A.L., Azam, F., Kirchman, D.L., Passow, U., Santschi, P.H., 2004. The oceanic gel phase: a bridge in the DOM–POM continuum. Mar. Chem. 92, 67–85. http://dx.doi.org/10.1016/j.marchem.2004.06.017.

Vogel, J.S., Southon, J.R., Nelson, D.E., Brown, T.A., 1984. Performance of catalytically condensed carbon for use in accelerator mass-spectrometry. Nucl. Instr. Meth. Phys. Res. Section B: Beam Interactions Mater. Atoms 5, 289–293.

Walker, B.D., Beaupré, S.R., Guilderson, T.P., Druffel, E.R.M., McCarthy, M.D., 2011. Large-volume ultrafiltration for the study of radiocarbon signatures and size vs. age relationships in marine dissolved organic matter. Geochim. Cosmochim. Acta 75, 5187–5202. http://dx.doi.org/10.1016/j.gca.2011.06.015.

Walker, B.D., Guilderson, T.P., Okimura, K.M., 2014. Radiocarbon signatures and size–age–composition relationships of major organic matter pools within a unique California upwelling system. Geochim. Cosmochim. Acta 126, 1–17. http://dx.doi.org/10.1016/j.gca.2013.10.039.

Walker, B.D., Beaupré, S.R., Guilderson, T.P., McCarthy, M.D., Druffel, E.R.M., 2016a. Pacific carbon cycling constrained by organic matter size, age and composition relationships. Nat. Geosci. http://dx.doi.org/10.1038/ngeo2830.

Walker, B.D., Griffin, S., Druffel, E., 2016b. Effect of acidified versus frozen storage on marine dissolved organic carbon concentration and isotopic composition. Radiocarbon. http://dx.doi.org/10.1017/RDC.2016.48.

Walker, B.D., Primeau, F.W., Beaupré, S.R., Guilderson, T.P., Druffel, E.R.M., McCarthy, M.D., 2016c. Linked changes in marine dissolved organic carbon molecular size and radiocarbon age. Geophys. Res. Lett. 43, 10,385–10,393. http://dx.doi.org/10.1002/2016GL070359.

Wang, X.C., Chen, R.F., Whelan, J., Eglinton, L., 2001. Contribution of “old” carbon from natural marine hydrocarbon seeps to sedimentary and dissolved organic carbon pools in the Gulf of Mexico. Geophys. Res. Lett. 28, 3313–3316.

Williams, P.M., Druffel, E.R.M., 1987. Radiocarbon in dissolved organic matter in the central North Pacific Ocean. Nature 330, 246–248.